

can Meteorological Society, in Tallahassee, in the fall of 1961. At that time several meteorologists commented that a pronounced Coriolis effect should not be expected for spirals of such small size when there is significant roughness.

The Kármán vortex trail (12) is of importance in turbulence theory. Vortices of this kind commonly form as a result of an adverse pressure gradient associated with sudden changes in channel depth or width, or with changes in velocity, or behind obstructions to fluid flow, especially in streams of water. Such vortices are easily seen when suitable tracer materials (aluminum chaff, dye, heavy floats) are put in the water. If flow past an obstacle is essentially symmetrical, two lines of vortices occur, one on each side of the wake. The two sets are staggered, so that no one vortex is directly opposite a vortex of the other set. The rotation in one set is opposite to that in the other, and there is a tendency for an upstream current to form between the two sets.

Outside of each vortex set, between it and the main stream of water, a spiral standing wave may develop. Within this wave there is an "up" motion on the side next to the vortex trail (the inside) and a "down" motion on the outside, as well as general longitudinal flow. Two such waves occur in strongly developed symmetrical flow behind an obstacle, one on each side, each presenting essentially a mirror image of the other. When viewed from above, the two waves combine to produce a clearly defined ogive pattern, with the point at, or immediately upstream from, the obstacle.

Along the side of a channel, behind a roughness element, a single vortex trail, with a single spiral wave outside it, may appear. If two spiral waves, developed from opposite channel walls, cross in midstream, a "rooster tail" (spout of water) is formed (13). Spiral waves on several scales have been observed, from small ones (measurable in centimeters) to large ones (measurable in tens of meters). They are responsible, in some instances, for the local transportation of sediment. They form at Froude numbers above $F = 1.0$, and at Reynolds numbers in the range $R = 120$ to $R = 4000$, when roughness is present. (No observations above $F = 3$ and $R = 4000$ were made.)

Spiral flow has been noted in two other connections. In one case, the flow appears to be a duplicate of Reiner's teapot effect (14); whether or not this is purely a surface-tension effect is not clear. In the other case the flow is a surface-tension feature which can be observed in tiny model streams flowing across waxed glass or heavily waxed paper. The surface-tension spiral produces an unstable meander-like pattern which changes position and appearance rapidly and erratically.

WILLIAM F. TANNER

*Geology Department,
Florida State University, Tallahassee*

References

1. S. Leliavsky, *Introduction to Fluvial Hydraulics* (Constable, London, 1959), pp. 95-147, 185-186.
2. A. Einstein and A. N. Harder, *Trans. Am. Geophys. Union* **35**, 114 (1954).
3. W. F. Tanner, *J. Geol. Educ.*, in press.
4. V. Kolar, *Rozpravy Cesk. Akad. Ved.* **66**, 105 (1956).
5. L. M. U. J. van Straaten, *J. Sediment. Petrol.* **21**, 47 (1951).
6. W. L. Stokes, *Bull. Geol. Soc. Am.* **68**, 1872 (1957).
7. W. F. Tanner, *Trans. Gulf Coast Assoc. Geol. Soc.* **12**, 295 (1962).
8. G. F. Jordan, *Science* **136**, 839 (1962).
9. R. A. Bagnold, *The Physics of Blown Sand and Desert Dunes* (Methuen, London, 1941), p. 176.
10. R. J. Kennedy and J. F. Fulton, ASME-EIC Hydraulics Conference paper No. 61-EIC-1 (1961).
11. M. Sibulkin, *J. Fluid Mech.* **14**, 21 (1962).
12. R. H. F. Pao, *Fluid Mechanics* (Wiley, New York, 1961), pp. 399-403.
13. J. F. Kennedy, *Calif. Inst. Technol., Rept. No. KH-R-2* (1961), p. 74.
14. M. Reiner, *Deformation, Strain and Flow* (Interscience, New York, 1960), p. 27.

18 October 1962

Mariner II: High-Energy-Radiation Experiment

The radiation experiment on Mariner II was undertaken to investigate (i) the dependence of the intensity of ionizing radiation in space upon distance from the sun; (ii) temporal variations of the radiation and their correlation with measurements of the magnetic field and plasma flux at the location of the spacecraft, and with solar-terrestrial disturbances; and (iii) the intensity and extent of magnetically trapped radiation, if any, around Venus.

A systematic dependence of radiation intensity upon distance from the sun is inferred from the observation that cosmic ray intensity at the earth is inversely correlated with solar activity throughout the 11-year solar cycle. Assuming that the cosmic radiation in

space far from the sun is constant, and that some of it is excluded from the region of the earth's orbit when the sun is active, one concludes that there is a region in which the radiation decreases as the sun is approached. It is of interest to know whether this decrease occurs in a restricted region beyond the earth's orbit or whether it occurs gradually so that there is a gradient near the earth.

The intensity and the time history of the increased charged-particle radiation which is observed at the earth immediately after some solar flares apparently depends upon (i) the character of the radiation ejected into space from the flare region; (ii) the location of the flare on the sun with respect to the earth; (iii) the distribution of the interplanetary magnetic field prior to ejection of the radiation from the sun; and (iv) the alterations in the interplanetary magnetic field caused by plasma ejected from the sun during and after the ejection of energetic charged particles.

Observation of solar-flare radiation and simultaneous observation of variations in plasma flux and the magnetic field at the spacecraft, outside of the geomagnetic field, will contribute to an understanding of these phenomena. In addition, measurements of the time required for radiation to propagate from the position of the spacecraft to the earth will be of interest.

If Venus has a magnetic field similar to the earth's, then it is to be expected that energetic charged particles are trapped in some regions around the planet. Measurement of both the magnetic field and the radiation near the planet can provide a better description of the planetary field than measurement of the magnetic field alone could provide.

Mariner II is well suited to the investigation of these phenomena. In approximately 100 days it travels from the earth, at 1.0 astronomical unit from the sun, to Venus, at 0.72 astronomical unit from the sun, remaining close to the plane of the ecliptic. Its attitude is completely stabilized so that the roll axis lies parallel to a radius vector from the sun at all times. Orientation about the roll axis is fixed so that the parabolic antenna, hinging on an axis perpendicular to the roll axis, can always point at the earth.

After being launched, the spacecraft falls behind the earth in its orbit; it later passes it, and when it meets Venus it is ahead of the earth. While passing,

it gradually turns 180° about its roll axis.

Three detectors were chosen for the experiment on high-energy radiation. These are a gas-filled integrating ionization chamber with a wall (0.2 g/cm²) of stainless steel; a thin-walled cylindrical glass Geiger-Müller (GM) tube shielded with stainless steel (the total thickness of the wall matches the thickness of the wall of the ionization chamber); and an identical glass Geiger-Müller tube shielded with beryllium of sufficient thickness to admit protons and heavier nuclei of the same energies as the protons and heavier nuclei admitted by the stainless-steel-shielded tube and the ion chamber. The two Geiger-Müller tubes differ in the efficiency with which they detect nonpenetrating electrons by the bremsstrahlung process. Table 1 gives further details concerning the detectors. The State University of Iowa has provided another radiation experiment, in which a thin-window Anton 213 Geiger-Müller tube is used.

The ionization chamber is read out continuously; the spacecraft samples the counting rate of the stainless-steel-shielded tube for 0.82 second and for 9.6 seconds every 443.4 seconds and the rate of the beryllium-shielded tube for the same time intervals every 887.0 seconds. The detectors are mounted close together in the forward structure of the spacecraft, well away from the principal mass of the vehicle. The axes of the Geiger-Müller tubes are perpendicular to the roll axis of the spacecraft and hence to the radius vector from the sun.

Figure 1 shows results from these detectors obtained during the first 28 days of operation. The data have been averaged to give about four values per day. The resulting statistical uncertainties are shown. The uncertainty associated with the ion chamber is the variation seen when the instrument is exposed to gamma rays in the laboratory. It may be remarked that the observed long-term drifts are within ±1 percent for the ion chamber and ±5 percent for the Geiger-Müller tubes.

The rate of ionization is typically 670 ion pairs per cubic centimeter per second per atmosphere of air (standard temperature and pressure), and the average omnidirectional flux measured by the stainless-steel-shielded Geiger-Müller tube is 2.95 particles per square centimeter per second. Hence, the average specific ionization, if isotropy is

Table 1. Characteristics of Mariner II radiation detectors.

Detector	Shielding	Corresponding energy of penetration (Mev)	Geometric factor	Dynamic range of counting rate* (counts/sec)
Integrating ion chamber	Stainless steel (0.2 g/cm ²)	Protons, $E > 10$; electrons, $E > 0.5$	Argon (1 lit.) at pressure of 4 atm; 10 ⁻¹⁰ coulomb per count; sensitive volume is sphere, 12.5 cm in diameter	10 ⁻³ to 10 ² = 3.4 × 10 ³ to 3.4 × 10 ⁷ ion pairs/cm sec atm of air†
Stainless-steel-shielded GM tube	Glass (0.030 g/cm ²) + stainless steel (0.160 g/cm ²)	Protons, $E > 10$; electrons, $E > 0.5$	6.97 cm ² omnidirectional	15 to 45,000
Beryllium-shielded GM tube	Glass (0.030 g/cm ²) + beryllium (0.113 g/cm ²)	Protons, $E > 10$; electrons, $E > 0.5$	6.91 cm ² omnidirectional; sensitive volume of GM tubes is approximately a cylinder, 1.3 cm in diameter, 6.0 cm long	15 to 45,000

* Minimum rates are those expected from galactic cosmic rays; maximum rates are determined by the instruments' responses. † Standard temperature and pressure.

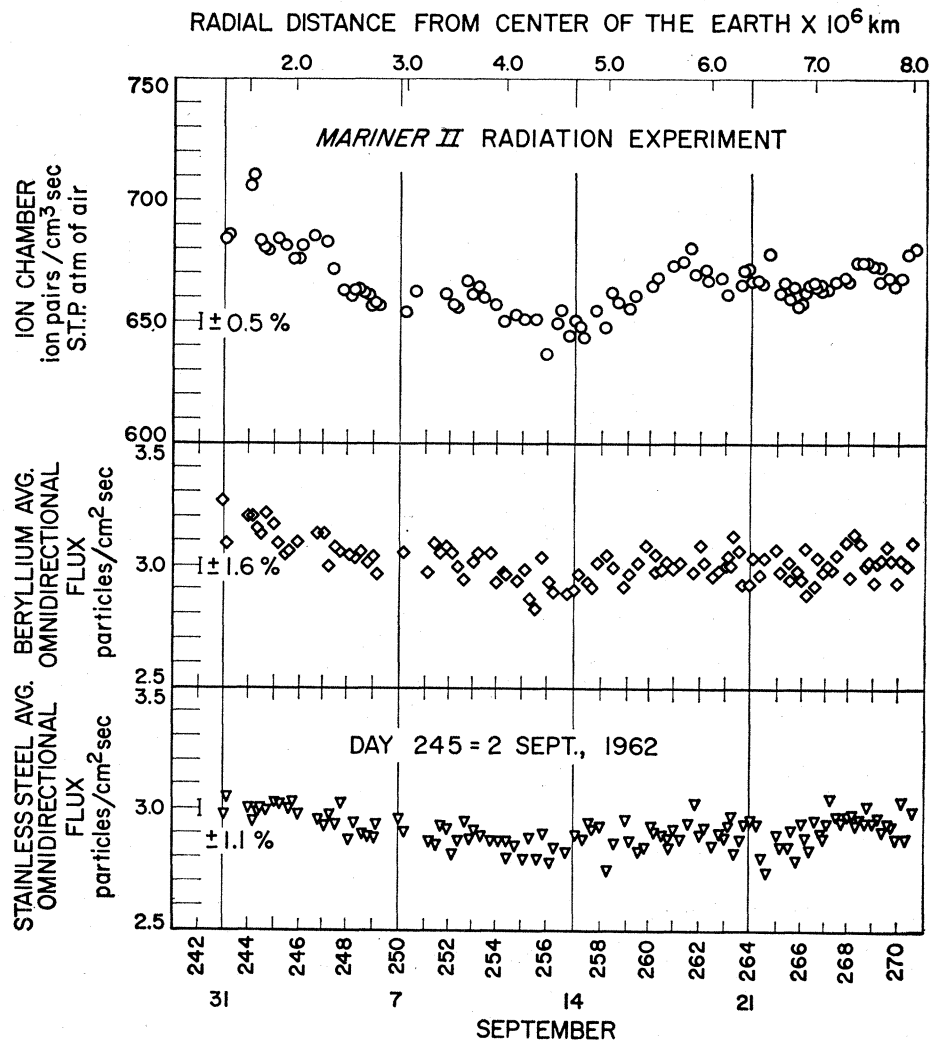
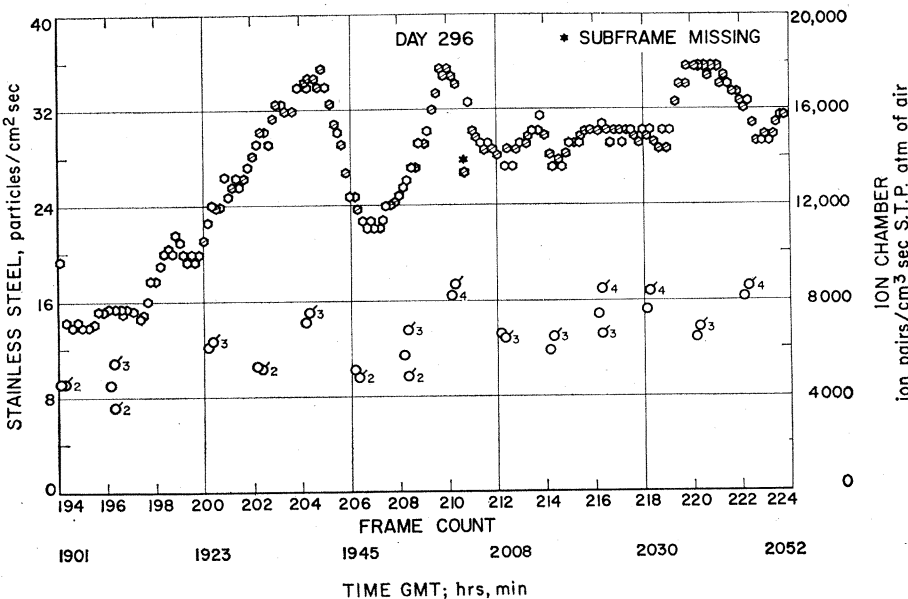
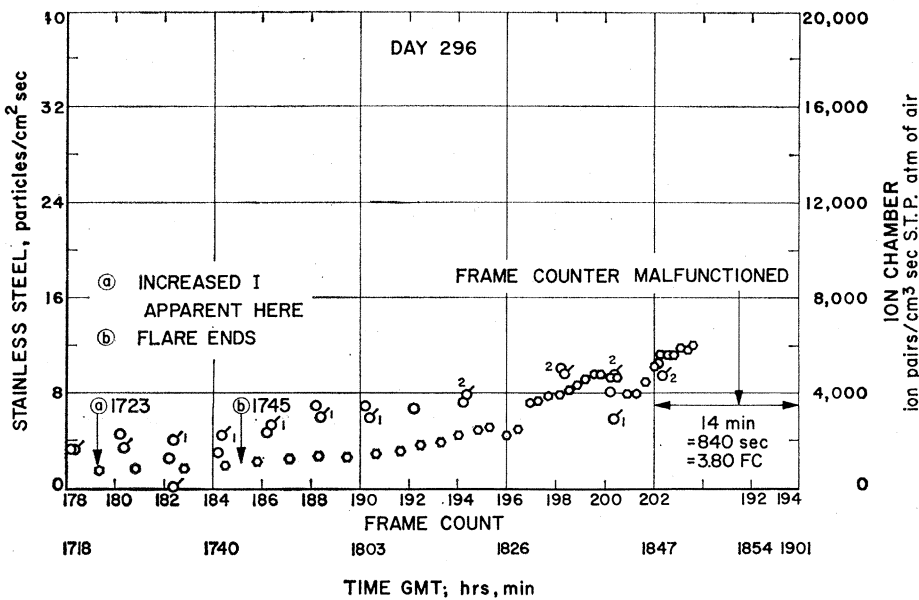
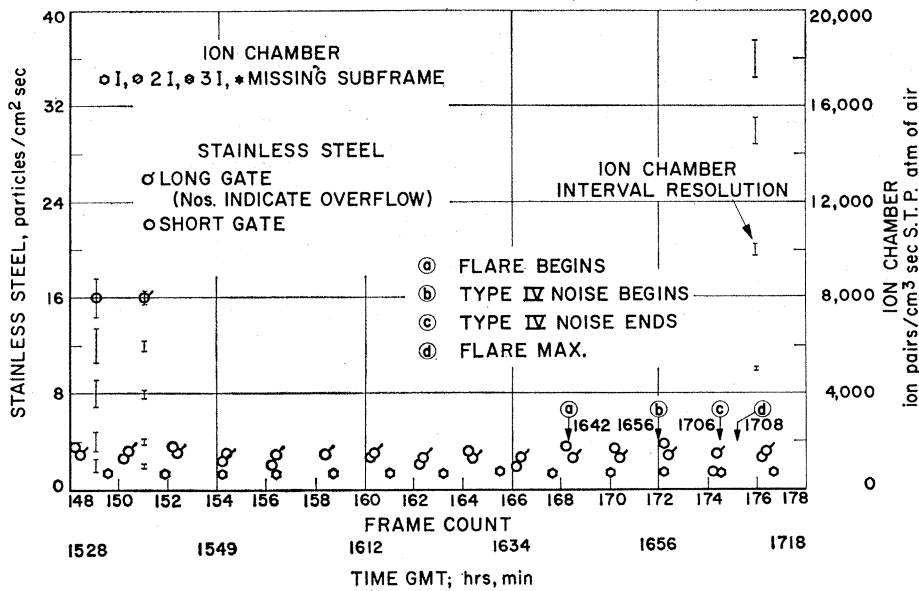


Fig. 1. The radiation in space measured by two Geiger-Müller counters and an argon-filled ionization chamber on Mariner II during the first 28 days of operation. The statistical uncertainties of the Geiger-Müller tube data and the variation of the ion-chamber response to gamma radiation are given at left.

MARINER II RADIATION EXPERIMENT DAY 296, OCTOBER 23, 1962



assumed, is 227 ion pairs per centimeter of air (standard temperature and pressure); this is 3.3 times the rate of energy loss by ionization calculated for a minimum ionizing proton. [The ionization rate agrees approximately with that measured by ion chambers in July and August, 1962, at high altitudes and high latitudes (1).] These data have not been corrected for the presence of the spacecraft mass.

The flux calculated from the beryllium-shielded tube is slightly higher than that deduced from the stainless-steel-shielded tube, but this difference is not considered significant.

The ion chamber recorded what may be a small Forbush decrease on 4 September, followed by a further decrease; return to a more constant level was recorded on 11 September. The relationship of these changes to results from a terrestrial neutron monitor is being studied.

The data received since 27 September are of the same character as those shown in Fig. 1 except for data received on 23 and 24 October, when a large increase was observed after a flare near the western limb of the sun. Figure 2 shows data obtained during the early part of this increase. (The spacecraft was 15.4 million km from the earth and 134.1 million km from the sun on 23 October.) The Sun-Earth-probe angle was 17.3°. The sequence of events was reported in the High Altitude Observatory (Boulder, Colorado) with preliminary reports essentially as follows.

1) Flare observed on 23 October near the western limb of sun. Beginning, 1642 hours; peak, 1708 hours; end, 1745 hours. Type IV noise observed from 1656 to 1706 hours.

2) Ionization had increased by 6.3 percent at 1723 hours. A more thorough analysis of the data will define the time of onset more accurately.

3) Ionization increased steadily to 17,000 ion pairs per cubic centimeter per second per atmosphere (standard temperature and pressure) by 1938 hours and fluctuated between 15,000 and 18,000 ion pairs until 2204 hours.

Fig. 2. Average omnidirectional flux and the rate of ionization measured by a Geiger-Müller counter and an argon-filled ion chamber on Mariner II, 15.4 million km from the earth on 23-24 October 1962. The statistical uncertainties in the Geiger-Müller tube data are indicated at left. Uncertainty in the ionization data results from the time-interval resolution of the read-out system.

The average omnidirectional flux varied from 10 to 16 particles per square centimeter per second during this time, so that the average specific ionization was of the order of 1200.

4) After 2204 hours the ionization and flux declined. The ionization may be described by $e^{-t/\tau}$; τ had three distinct values during the period 23 October, 2204 hours, to 24 October, 2053 hours. At the latter time the ionization was 1080, or 61 percent above normal.

We suggest that this radiation was associated with the flare described. It is interesting to note that, according to the High Altitude Observatory preliminary reports, there were six class-2 flares from 24 August to 8 November, of which only the one on 23 October and one on 7 September at 1535 hours produced type IV radio noise. The flare of 7 September occurred in the eastern hemisphere of the sun and produced no radiation detected by the Mariner II experiment.

The data have not yet been thoroughly analyzed, and at present only preliminary geomagnetic and solar data are available. It is possible to state these tentative conclusions.

1) During the period 31 August to 15 November the radiation detected behind a 0.2 g/cm² absorber was approximately constant except for the period 23–24 October. The levels are

about those expected for the galactic cosmic radiation at this part of the solar cycle. Measurements were made at ranges 0.5 million to 27.6 million km from the center of the earth during this time.

2) On 23 October, beginning at 1723 hours, the rate of ionization increased to a maximum approximately 26 times background cosmic radiation. Unusually high radiation was still detected at 2053 hours on 24 October. This radiation is probably associated with a class-2 flare and type IV radio noise which occurred on the western limb of the sun prior to the increase. Of six class-2 flares reported by the High Altitude Observatory during the period of observation, only this one produced a detectable increase in radiation (3).

HUGH R. ANDERSON

Jet Propulsion Laboratory,
California Institute of Technology,
Pasadena

Notes

1. H. V. Neher, private communication.
2. *High Altitude Observatory Preliminary Report of Solar Activity, TR582* (26 Oct. 1962).
3. I thank L. Parker, L. Lewyn, N. Yamane, and J. Shepperd of the Jet Propulsion Laboratory for constructing the instruments described and for integrating them into the Mariner spacecraft. Professor H. V. Neher of the California Institute of Technology and Professor J. A. Van Allen and Mr. L. Frank of the State University of Ohio helped me calibrate the instruments and offered valuable comments on the experiment.

10 December 1962

The Stump-Tailed Macaque: A Promising Laboratory Primate

Abstract. *Members of Macaca speciosa have characteristics that make them suitable primates for neuropsychological investigation. They work well in discrimination training, have a varied behavioral repertoire and social interaction, and seem to be at least as intelligent as M. mulatta. They are docile and submit readily to laboratory routine.*

The nonhuman primate most commonly used in research today is the rhesus monkey, *Macaca mulatta*. It is readily obtained, is relatively hardy, and has a varied repertoire of behavior. There is now available a large body of normative data concerning its anatomy, development, and behavior. However, the rhesus monkey is belligerent, and this complicates handling. It would therefore be of considerable value to have available a laboratory primate of milder disposition that possesses the advantages of *M. mulatta*.

During studies of somatic and behavioral development in monkeys we have made observations on ten monkeys, of a species commonly known as

the stump-tailed macaque, that are of various ages (up to 4 years) and are remarkably docile and manageable. This species thrives in the laboratory, withstands surgical procedures well, and makes an excellent subject for behavioral investigation. In this report we offer a behavioral description of this docile species of macaque.

Anderson (1), in his 1878 account of two expeditions to western Yunnan, China, proposed the scientific title *Macaca arctoides* for the stump-tailed macaque. On the other hand, Allen (2) placed this monkey within the genus *Lyssodes* along with *M. mulatta* and *M. irus*, and designated the species *macacus speciosus*. In accordance with

the modern designation of the popular macaques, we have adopted the scientific name *Macaca speciosa* for the stump-tailed macaque. This species is similar to the Japanese macaque, *M. fuscata*, but should be differentiated from the pig-tailed macaque, *M. nemestrina*.

Macaca speciosa ranges from northern India, Tibet, and western China down through Burma to the Indochina peninsula (2). Its natural habitat is said to be hill and mountain regions where temperature may fall below zero (3).

Macaca speciosa is a large, red-faced monkey in which the tail is a 1-inch stump. The coat is heavy and varies in color from greenish brown in the adult to chocolate brown in the young. The cheeks vary in pigmentation from bright red to pale pink, and there are black freckled areas around the nose of the adult. Comparison of the crown-rump length and the weight of our ten monkeys with data reported by Van Wagenen and Catchpole (4) for *M. mulatta* revealed no consistent differences.

The skull of *M. speciosa* differs in certain respects from that of *M. mulatta*. *Macaca speciosa* has larger mandible and maxilla and a more pronounced prognathism. Measurements of the cranial cavity reveal that the A-P axis is somewhat shorter than in *M. mulatta*, but the values are within the range of normal variability for *M. mulatta*, as reported by Olszewski (5). A gross examination of the fissural pattern on the brain surface revealed no marked differences in the two species. Our studies of the brain to date suggest that the available stereotaxic atlases for *M. mulatta* (5, 6) could be employed for subcortical electrode placements in *M. speciosa*.

The salient feature of the behavior of *M. speciosa* is docility toward man. In the home cage, the animal often solicits scratching, stroking, and rubbing from humans by pushing up against the cage bars and extending a limb. If the cage door is opened, the monkey may timidly withdraw but will not seriously resist being picked up. Like the young chimpanzee, the immature monkey may even jump into the handler's arms, clutch tightly, and make pelvic thrusts. Though there is no malice on the part of the monkey, we have found it wise to wear a laboratory coat to avoid being scratched. Pinning the monkey's arms behind its back, an